

Preparation and properties of Pd/Ag composite membrane for direct synthesis of hydrogen peroxide from hydrogen and oxygen

Li Wang^{*}, Shiguo Bao, Jianhua Yi, Fei He, Zhentao Mi

Key Laboratory for Green Chemical Technology of the Ministry of Education, School of Chemical Engineering and Technology, Tianjin University, Tianjin 300072, PR China

Received 14 December 2006; received in revised form 6 October 2007; accepted 11 October 2007

Available online 22 October 2007

Abstract

Pd and Pd–Ag alloy membranes on porous alumina tubes were prepared by means of simultaneous and sequential electroless plating technique. The characterizations of Pd–Ag composite membranes were performed using scanning electron microscopy (SEM), X-ray diffractometer (XRD) and X-ray photoelectron spectroscopy (XPS). The catalytic reaction of H₂ and O₂ to directly form hydrogen peroxide was carried out in the membrane reactor at 293 K. The thickness of Pd–Ag alloy membranes obtained by simultaneous electroless plating was thinner than that by sequential electroless plating. And high uniformity of grains was found on the surface of the Pd–Ag membrane prepared by simultaneous electroless plating. The concentration of H₂O₂ increased with the increase in transmembrane pressure differences of hydrogen and a high concentration of H₂O₂ was obtained on the membrane which consists of a Pd layer on the surface of the membrane and a Pd–Ag alloy layer inside the membrane.

© 2007 Elsevier B.V. All rights reserved.

Keywords: Hydrogen peroxide; Pd–Ag composite membrane; Direct synthesis; Membrane reactor

1. Introduction

Hydrogen peroxide is widely accepted as a green oxidant and, today, is almost exclusively produced by the sequential hydrogenation and oxidation of an alkyl-anthraquinone known as the AQ process [1]. However, there are problems associated with the AQ process and these include the cost of the working solution and the requirement for periodic replacement of anthraquinone due to its degradation [2]. In addition, this process involves a number of steps, including extraction of H₂O₂ from organic working solution to the aqueous phase and purification of the raw aqueous H₂O₂ in order to remove organic contaminants. Hence, direct synthesis would be a more economic, simple and environmentally friendly alternative route.

In the last 5 years considerable progress in the research of the direct synthesis of hydrogen peroxide from hydrogen and oxygen has been achieved. The researches deal with several

aspects such as the preparation, the characterization and the performance of catalysts, the role of promoters and solvents, and the reaction mechanism [3–19]. However, to date the potential risk in the production due to the formation of explosive H₂/O₂ mixtures which has a extremely broad explosion region (4.65–93.9 vol.% hydrogen in oxygen at atmosphere) is an obstacle to its industrial application. The process of the direct synthesis can use H₂/O₂ mixtures away from the explosive region to ensure safety. For example, the pilot plant for direct synthesis of hydrogen peroxide, as a dilute solution in methanol and an intermediate product for manufacturing propylene oxide, operates below the explosion limit [20]. However, a low partial pressure of hydrogen is unfavorable for the process of the direct synthesis because there is a great excess of oxygen in the reactor and a lower mass transfer rate for H₂ at the gas–liquid interface.

Recently, the use of specially designed membranes for the synthesis of hydrogen peroxide from H₂ and O₂ has attracted considerable interest because it provides a promising approach to overcoming the problem of safety [21–24]. Strukul and co-workers [21–23] prepared palladium and palladium/platinum bimetallic catalytic membranes for the

^{*} Corresponding author. Tel.: +86 22 27892340; fax: +86 22 27402604.

E-mail address: wlytj@yahoo.com.cn (L. Wang).

direct synthesis. They found that the latter gave higher productivity and selectivity. However, there is a high degree of H_2O_2 decomposition over both the palladium and palladium/platinum bimetallic catalytic membranes. Choudhary and co-workers [24] reported a hydrophobic composite Pd-membrane catalyst which includes a hydrophobic polymer layer for the direct synthesis. The role of the hydrophobic polymer layer is to promote desorption of H_2O_2 from the surface of the membrane [19]. However, there is a significant decomposition of H_2O_2 on the membrane.

The aim of this work is to investigate the preparation and the fabrication of the palladium–silver alloy membranes on alumina tubes that control the performance of the membrane catalyst for the direct synthesis. Effects of the transmembrane pressure difference of hydrogen on the concentration of H_2O_2 and H_2 permeance were also studied.

2. Experimental

2.1. Materials

Porous α -alumina tubes (Nanjing Jiushi High-Tech Co. Ltd., China) with average pore size of 150 nm were used as membrane support. The tubes were 250 mm in length with an outside diameter of 12 mm and an inside diameter of 7 mm. Prior to the activation, the tubes were cleaned by sequential washing with methanol, hydrochloric acid (4.5 wt.%) and deionized water under ultrasonic irradiation.

2.2. Activation of supports

The activation procedure consisted of a two-step immersion sequence, which was in acidic SnCl_2 solution (sensitization solution) followed by acidic PdCl_2 solution (activation solution) [25]. Typically, the alumina tube was first immersed in the sensitization solution for 5 min and cleaned by deionized water, and then was immersed in the activation solution for 5 min and cleaned by deionized water. This cycle was repeated 10 times. The compositions of the sensitization and the activation solutions are shown in Table 1.

Table 1
Composition of sensitization and activation baths

Plating method	Sensitization solution		Activation solution	
	SnCl_2 (g/L)	HCl (37 wt.%) (mL/L)	PdCl_2 (g/L)	HCl (37 wt.%) (mL/L)
Plating Pd and Ag sequentially	1	2.5	3	2.5
Plating Pd and Ag simultaneously	3	5	5	5

Table 2
Composition of electroless plating baths and conditions of electroless plating

Plating method	PdCl_2 (g/L)	AgNO_3 (g/L)	Na_2EDTA (g/L)	NH_4OH (mL/L)	$\text{N}_2\text{H}_4\cdot\text{H}_2\text{O}$ (mL/L)	PH	Temperature (K)
Pd plating	4	0	70	500	10	10	338
Ag plating	0	1	35	500	5	10	328
Plating Pd/Ag simultaneously	3	0.8	70	500	12	10	333

2.3. Deposition of Pd and Ag by electroless plating

The deposition of Pd and Ag on the activated alumina tube was performed using a sequential electroless plating of Pd and Ag (i.e., Pd plating followed by Ag plating) or simultaneous plating of both metals. The compositions and temperature of the plating baths are shown in Table 2. The deposition procedure lasted 3 h and was repeated two times. After deposition, the as-deposited membrane was rinsed with deionized water and then activated under hydrogen atmosphere for 4 h at 1073 K for the sequential electroless plating and at 773 K for the simultaneously electroless plating, respectively.

2.4. Membrane characterization

The morphology and microstructure of the Pd–Ag membrane were measured by an environmental scanning electron microscopy (ESEM, Philips XL-30) equipped with an energy dispersive spectrometer (EDS). X-ray diffraction patterns of the Pd–Ag membranes were recorded with a Rigaku D-max 2500 V $\text{K}\alpha$ radiation source (40 kV, 200 mA). XPS spectra of the Pd–Ag membrane were obtained with a PHI 1600 X-ray photoelectron spectroscopy (Perkin-Elmer Inc.) using $\text{Mg K}\alpha$ (1253.6 kV, 300 W) as the excitation source. The $\text{Al}(2p)$ peak, at 74.4 eV, was taken as reference in accounting effects, and the analyzed sample area was 0.8 mm^2 .

2.5. Catalytic test and gas permeation measurements

Catalytic reactions were carried out at 293 K in a semi-batch reactor in which the membrane was sealed in a tubular holder (see Fig. 1). Typically, 12 mL methanol and 2 mg phosphoric acid were added to the reactor. H_2 was continuously fed to the bottom of the reactor from the shell side through the mass flow controller at flow rate of 1 mL min^{-1} . Oxygen at flow rate of 10 mL min^{-1} controlled by mass flow controller was continuously passed through a bubbler containing methanol, then to the tube side of the membrane reactor, to prevent excessive evaporative loss of the organic solvent from the reactor.

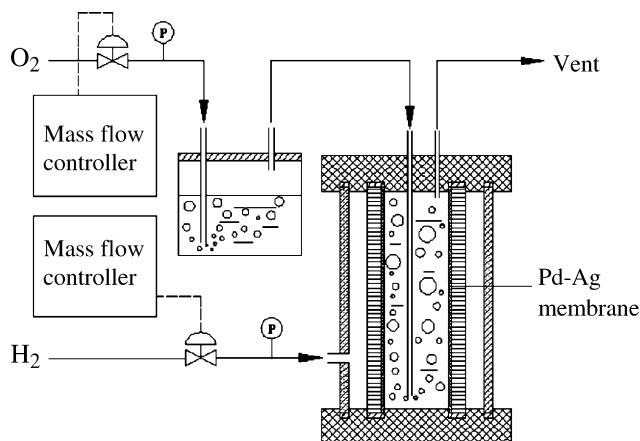


Fig. 1. Schematic diagram of membrane reactor.

Hydrogen peroxide concentration was determined by the iodometric titration.

H₂ permeation measurements were conducted on the Pd–Ag composite membranes at 293 K temperature with the same apparatus. The upstream pressure was controlled by a back-pressure regulator, whereas the downstream gas was vented to air. The permeation rates of hydrogen were measured by a mass flowmeter.

3. Results and discussion

3.1. Surface morphology of membranes

It is well known that the electroless deposition of silver needs to be initiated by Pd nuclei [26]. This means that pure Ag deposition or simultaneous Pd–Ag deposition cannot be directly fulfilled on these unmodified substrates. Therefore,

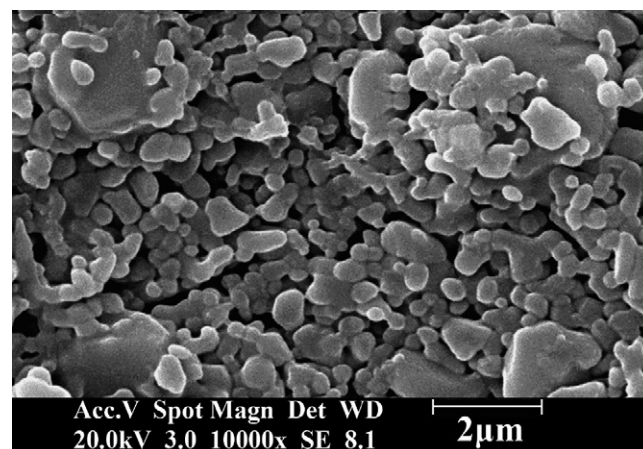


Fig. 2. SEM of surface of alumina tube after activation.

pre-deposition of the palladium membrane was performed on the α -Al₂O₃ tube to solve the problems [27]. Fig. 2 shows the scanning electron micrographs after activation of the alumina tube. As observed by SEM, after surface activation, palladium nuclei have been doped on the support surface. But they are not uniform in size and distribution.

Fig. 3 shows the SEM micrograph of the Pd–Ag membrane prepared by sequential electroless plating during its formation process. A significant change in the surface morphology of the Pd–Ag membrane was found in this process. After depositing Pd only, the size distribution of Pd particles became broader on the top layer of the support surface (see Fig. 3a). This might be ascribed to that part of the palladium was deposited on the initial nuclei formed in the activation process and the others directly fulfilled on the unactivated support. After depositing Ag sequentially, the size of particles became larger further and size distribution became uniform because Ag was deposited on

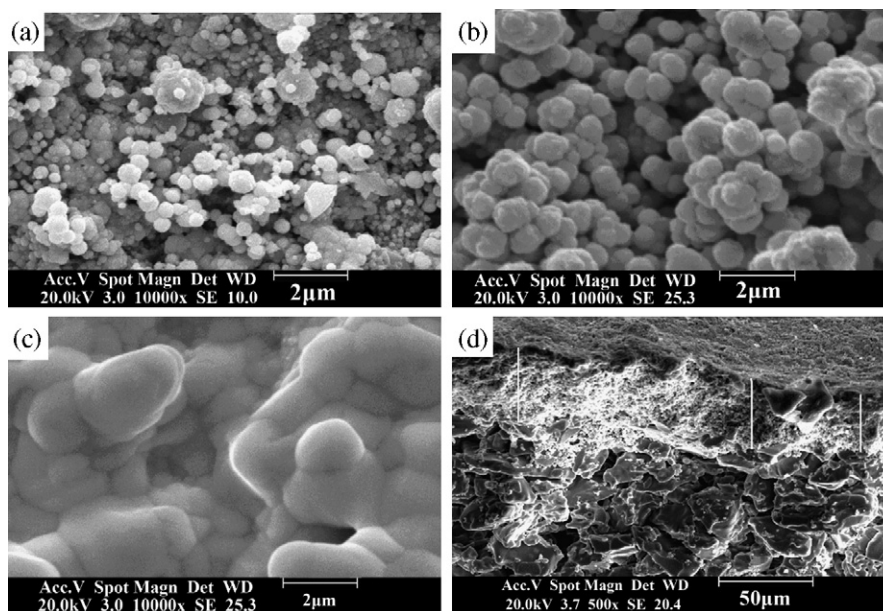


Fig. 3. SEM of Pd–Ag membrane by sequential electroless plating. (a) surface after depositing Pd only, (b) surface after depositing Ag sequentially, (c) surface after annealing at 1073 K, (d) cross-section after annealing at 1073 K.

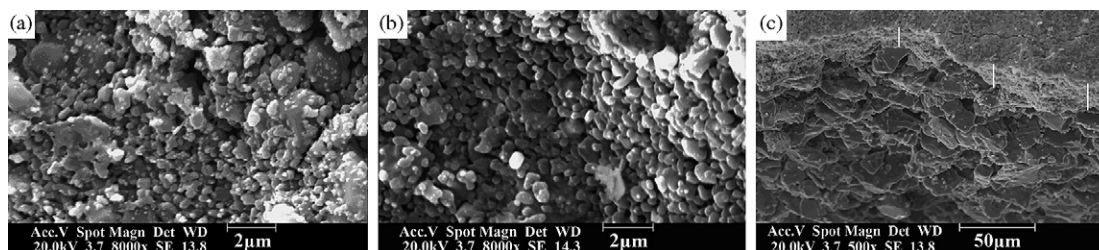


Fig. 4. SEM of surface of Pd/Ag membrane by simultaneous electroless plating. (a) surface after co-depositing Pd and Ag, (b) surface after annealing at 773 K, (c) cross-section after annealing at 773 K.

the Pd nuclei formed in the Pd deposition process. After annealing at 1073 K (see Fig. 3c), an obvious dense layer was found on the surface of the support. The average thickness of the Pd–Ag layer on the α - Al_2O_3 tube was about 37.5 μm . In our work, the average value of thickness of the membranes is calculated by three estimated obtained from different locations on the membrane sample from the SEM photographs after annealing in all cases.

Fig. 4 shows the SEM micrograph of the Pd–Ag membrane prepared by simultaneous electroless plating during its formation process. Apparently, the surface morphology of the membrane prepared by simultaneous electroless plating appears uniform and smooth with few large grains on the surfaces before and after annealing at 773 K compared to the sample prepared by simultaneous plating. The average thickness of the Pd–Ag layer was about 15.7 μm . This thickness was much less than that of the sample by sequential electroless plating.

3.2. Surface state and composition of membranes

The XRD pattern of Pd–Ag membrane obtained after annealing at 773 K is shown in Fig. 5. There are reflection peaks at $2\theta = 40.1^\circ$, 46.18° and 67.02° , corresponding to the alloy phase of Pd–Ag in the membrane.

Further analysis of Pd–Ag membranes were performed using XPS. The Pd(3d) and Ag(3d) spectra obtained from two membranes after annealing are shown in Fig. 6. The binding

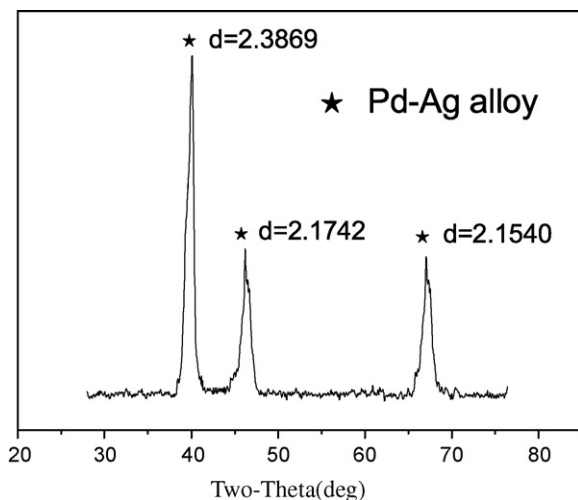


Fig. 5. XRD pattern of Pd–Ag membrane obtained after annealing at 773 K.

energies of 335.1 and 340.1 eV correspond to the $3d_{5/2}$ and $3d_{3/2}$ states of metallic palladium. The similar energies of 335.6 and 341.0 eV for the simultaneous plating sample, and of 335.4 and 340.7 eV for the sequential plating sample indicate metallic palladium existed on the Pd–Ag surface. The binding energies for Ag($3d_{5/2}$) and Ag($3d_{3/2}$) are at 367.5 and 373.4 eV, respectively. The results observed on surface of two samples indicate that Ag is not oxidized and present mainly as metallic silver.

Two methods (EDS and XPS) were used to determine the amounts of Pd and Ag deposited on the membrane supports after annealing. The quantitative analysis results of the membrane surface composition are summarized in Table 3. It is observed that the analysis results of Pd/Ag ratio on the surface of the membrane are strongly dependent on the analysis technique used. For the sample by simultaneous electroless plating, the Pd/Ag ratio is 1:1 (in at.%) by EDS, but 3:1 (in at.%) by XPS. The XPS technique is highly surface specific and its measurement depth is 2 nm below the top surface. The depth of scan by EDS is 1 μm below the top surface. And thus, the analytic data obtained by EDS can be considered the bulk composition of the specimen. The results mentioned above for the sample of simultaneous plating indicated that the membrane composition along the depth was not uniform and the top surface of the membrane was rich in Pd. This result agrees with

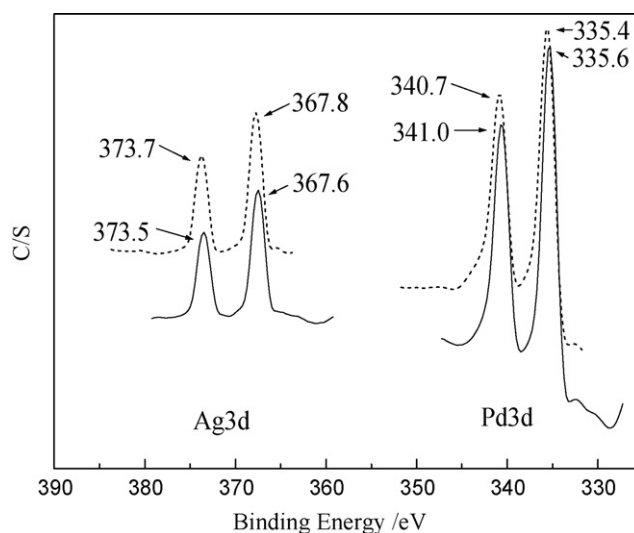


Fig. 6. XPS spectra of Pd–Ag membrane after annealing. Sample 1 (—) by simultaneous plating, sample 2 (- - -) by sequential plating.

Table 3
Composition of Pd–Ag membranes

Sample	Pd (at.%)		Ag (at.%)		Pd/Ag	
	By EDS ^a	By XPS	By EDS ^a	By XPS	By EDS	By XPS
Plating Pd/Ag simultaneously	17.32	8.9	13.12	2.8	1	3
Plating Pd/Ag sequentially	5.87	4.6	0.440	1.2	13	4

^a Average value calculated by five measurements obtained from different locations on the membrane samples.

the observations by other investigators, although the contradictory result, i.e., surface enrichment in silver, was also published for Pd–Ag alloy [28,29]. A similar result was obtained on the surface of the sample prepared by sequential electroless plating of Pd and Ag (i.e., Pd plating followed by Ag plating). According to the procedure of the preparation, a result of silver enrichment should occur on the top surface of this sample because Ag deposition proceeds last. However, the Pd/Ag ratio of the sample obtained by sequential electroless plating is 4:1 by XPS (see Table 3). These analysis results indicate that a diffusion of the bulk palladium towards the surface occurs during annealing.

For the sample obtained by sequential plating, the Pd/Ag ratio is 13:1 by EDS indicating a lack of silver in this membrane bulk. This result indicated that the bi-layered phenomenon occurred in the membrane obtained by sequential electroless plating.

3.3. Catalytic activity

Fig. 7 summarizes the results on the concentration of H₂O₂ using different membrane catalysts. Compared to the membrane catalyst obtained by sequential electroless plating (Pd–Ag/α–Al₂O₃ (seq)), the relatively low concentration of H₂O₂ was found over the Pd–Ag membrane obtained by simultaneous electroless plating (Pd–Ag/α–Al₂O₃ (sim)) because its thickness is thinner. This indicated that the membrane thickness was a crucial parameter which had a beneficial effect on the catalytic performance of the membranes. Ag in the Pd-base

membrane is essential to can improve the resistance of the hydrogen embrittlement and H₂ permeation of the Pd-based membranes. However, the results of the direct synthesis of H₂O₂ over supported powder catalysts indicate that supported Pd and Pd–Au alloy catalysts are highly effective [30]. Therefore, to enhance the catalytic performance of the membranes, another Pd layer with the thickness of 2–3 μm was added to both Pd–Ag/α–Al₂O₃ (seq) and Pd–Ag/α–Al₂O₃ (sim) by electroless plating. Two membrane catalysts thus obtained were Pd/Pd–Ag/α–Al₂O₃ (seq) and Pd/Pd–Ag/α–Al₂O₃ (sim). It was found that the concentration of H₂O₂ over both Pd/Pd–Ag/α–Al₂O₃ (seq) and Pd/Pd–Ag/α–Al₂O₃ (sim) increased compared to the membranes of Pd–Ag layer only. These results indicated the Pd layer was highly effective for the direct synthesis of H₂O₂ from H₂ and O₂. This trend in catalytic performance of Pd membranes is consistent with the results over the supported palladium powder catalysts, although the catalytic performance of the membrane catalysts is lower than that of the supported Pd-based powder catalysts, which can give more than 1 wt.% concentration of H₂O₂ at optimized reaction conditions.

Furthermore, the concentration of H₂O₂ was higher over Pd/Pd–Ag/α–Al₂O₃ (sim) than Pd/Pd–Ag/α–Al₂O₃ (seq) (Fig. 7). There was a significant difference in the H₂ permeated flux between Pd/Pd–Ag/α–Al₂O₃ (seq) and Pd/Pd–Ag/α–Al₂O₃ (sim) at the same transmembrane pressure. For example, the H₂ permeated flux were 0.9 mL cm^{−2} min^{−1} for Pd/Pd–Ag/α–Al₂O₃ (sim) and 0.2 mL cm^{−2} min^{−1} for Pd/Pd–Ag/α–Al₂O₃ (seq).

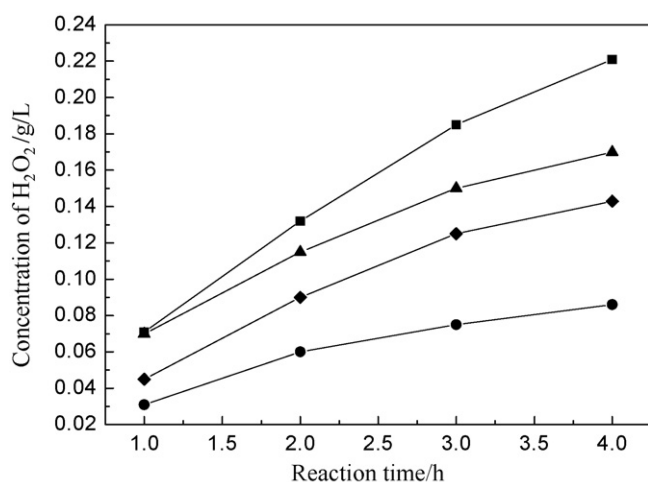


Fig. 7. Concentration of H₂O₂ over different membrane catalysts. (■) Pd–Pd–Ag/α–Al₂O₃ simultaneously, (●) Pd–Ag/α–Al₂O₃ simultaneously, (▲) Pd/Pd–Ag/α–Al₂O₃ sequentially, (◆) Pd–Ag/α–Al₂O₃ sequentially.

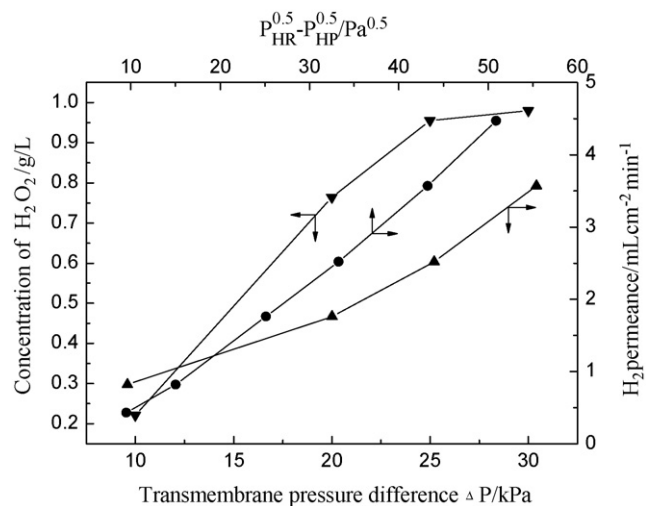


Fig. 8. The effect of transmembrane pressure difference on the H₂O₂ concentration and H₂ permeated flux. (●) Concentration of H₂O₂. (▲) Flux of hydrogen. Pd/Pd–Ag/α–Al₂O₃ (sim). reaction time = 4 h.

(seq). The accordant relationship between the concentration of H_2O_2 and the permeation of H_2 indicated that the H_2 permeated flux had a significant effect on the catalytic reaction of H_2 and O_2 to form H_2O_2 .

The effects of transmembrane pressure on the concentration of H_2O_2 and H_2 permeated flux were also investigated (Fig. 8). The hydrogen flux increased with increasing transmembrane pressure differences. This is consistent with the solution–diffusion mechanism of hydrogen through palladium membranes. Under this condition, the hydrogen flux should display a linear dependence on the difference of the square roots of inside and outside pressures [31]. This is confirmed in Fig. 8 for the Pd/Pd–Ag/ α - Al_2O_3 composite membrane. At low transmembrane pressure differences, the concentration of H_2O_2 increases with increasing transmembrane pressure differences. However, above 25 kPa the concentration of H_2O_2 reaches a plateau, indicating that the influence of transmembrane pressure differences is minimized. The diffusion rate of hydrogen in the membrane increased with increasing the transmembrane pressure differences, resulting in the increase in the quantity of hydrogen activated on the surface of the membrane. It is reasonable to assume that the quantity of hydrogen activated was relatively large so that the mass transfer of O_2 at the gas–liquid interface or the surface reaction of hydrogen activated with oxygen adsorbed on the catalyst became the rate-controlling step at high transmembrane pressure differences.

4. Conclusions

It is possible to form hydrogen peroxide from H_2 and O_2 under mild conditions with a fair productivity using Pd–Ag/ α - Al_2O_3 ceramic composite membranes. The catalytic activity of the membranes depends on the thickness, surface state and surface composition of the membranes. Depositing another Pd layer on the Pd–Ag/ α - Al_2O_3 membrane obtained by simultaneous electroless plating increases the concentration of H_2O_2 compared with the membrane of Pd–Ag layer containing only. The membrane catalyst with a Pd–Ag layer obtained by simultaneous plating inside and another Pd layer (Pd/Pd–Ag/ α - Al_2O_3) on the outside gave the highest concentration of H_2O_2 .

Acknowledgements

The authors gratefully acknowledge financial support provided by National Natural Science Foundation of China (Grant No. 20446003) and the PhD Special Foundation of the Ministry of Education (Grant No. 20030056035).

References

- [1] W. Gerhartz, fifth ed., *Ullmann's Encyclopedia of Industrial Chemistry*, vol. A13, VCHm, Weinheim, 1988, pp. 443–446.
- [2] A. Drelinkiewicz, A. Pukkinen, R. Kangas, R. Laitinen, *Catal. Lett.* 94 (2004) 157–170.
- [3] B.E. Solsona, J.K. Edwards, P. Landon, A.F. Carley, A. Herzing, C.J. Kiely, G.J. Hutchings, *Chem. Mater.* 18 (2006) 2689–2695.
- [4] G. Li, J. Edwards, A.F. Carley, G.J. Hutchings, *Catal. Today* 114 (2006) 369–371.
- [5] S. Melada, R. Rioda, F. Menegazzo, F. Pinna, G. Strukul, *J. Catal.* 239 (2006) 422–430.
- [6] Y.-F. Han, J.H. Lunsford, *J. Catal.* 230 (2005) 313–316.
- [7] Y.-F. Han, J.H. Lunsford, *Catal. Lett.* 99 (2005) 13–19.
- [8] J.K. Edwards, B.E. Solsona, P. Landon, A.F. Carley, A. Herzing, C.J. Kiely, G.J. Hutchings, *J. Catal.* 236 (2005) 69–79.
- [9] J.K. Edwards, B. Solsona, P. Landon, A.F. Carley, A. Herzing, M. Watanabe, C.J. Kiely, G.J. Hutchings, *J. Mater. Chem.* 15 (2005) 4595–4600.
- [10] T. Ishihara, Y. Ohura, S. Yoshida, Y. Hata, H. Nishiguchi, Y. Takita, *Appl. Catal. A: Gen.* 291 (2005) 215–221.
- [11] S. Chinta, J.H. Lunsford, *J. Catal.* 225 (2004) 249–255.
- [12] M. Okumura, Y. Kitagawa, K. Yamaguchi, T. Akita, S. Tsubota, M. Haruta, *Chem. Lett.* 32 (2003) 822–823.
- [13] P. Landon, P.J. Collier, A.F. Carley, D. Chadwick, A.J. Papworth, A. Burrows, C.J. Kiely, G.J. Hutchings, *Phys. Chem. Chem. Phys.* 5 (2003) 1917–1923.
- [14] J.H. Lunsford, *J. Catal.* 216 (2003) 455–460.
- [15] R. Burch, P.R. Ellis, *Appl. Catal. B: Environ.* 42 (2003) 203–211.
- [16] D. Hancu, J. Green, E.J. Beckman, *Ind. Eng. Chem. Res.* 41 (2002) 4466–4474.
- [17] A.G. Gaikwad, S.D. Sansare, V.R. Choudhary, *J. Mol. Catal. A: Chem.* 181 (2002) 143–149.
- [18] V.R. Choudhary, A.G. Gaikwad, S.D. Sansare, *Catal. Lett.* 83 (2002) 235–239.
- [19] V.V. Krishnan, A.G. Dokoutchaev, M.E. Thompson, *J. Catal.* 196 (2000) 366–374.
- [20] <http://www.chemie.de/news/e/44266/>.
- [21] S. Melada, F. Pinna, G. Strukul, S. Perathoner, G. Centi, *J. Catal.* 237 (2006) 213–219.
- [22] S. Abate, G. Centi, S. Melada, S. Perathoner, F. Pinna, G. Strukul, *Catal. Today* 104 (2005) 323–328.
- [23] G. Centi, R. Dittmeyer, S. Perathoner, M. Reif, *Catal. Today* 79–80 (2003) 139–149.
- [24] V.R. Choudhary, A.G. Gaikwad, S.D. Sansare, *Angew. Chem. Int. Ed.* 40 (2001) 1776–1779.
- [25] R.S. Souleimanova, A.S. Mukasyan, A. Varma, *J. Membr. Sci.* 166 (2000) 249–257.
- [26] D.A.P. Tanaka, M.A.L. Tanco, S. Niwa, Y. Wakui, F. Mizukami, T. Namba, T.M. Suzuki, *J. Membr. Sci.* 247 (2005) 21–27.
- [27] J. Tong, L. Su, Y. Kashima, R. Shirai, H. Suda, Y. Matsumura, *Ind. Eng. Chem. Res.* 45 (2006) 648–655.
- [28] L. Yang, Z. Zhang, X. Gao, Y. Guo, B. Wang, O. Sakai, H. Sakai, T. Takahashi, *J. Membr. Sci.* 252 (2005) 145–154.
- [29] T. Huang, M. Wei, H. Chen, *Sep. Purif. Technol.* 32 (2003) 239–245.
- [30] P. Landon, P.J. Collier, A.J. Papworth, C.J. Kiely, G.J. Hutchings, *Chem. Commun.* (2002) 2058–2059.
- [31] D. Yepes, L.M. Cornaglia, S. Irusta, E.A. Lombardo, *J. Membr. Sci.* 274 (2006) 92–101.